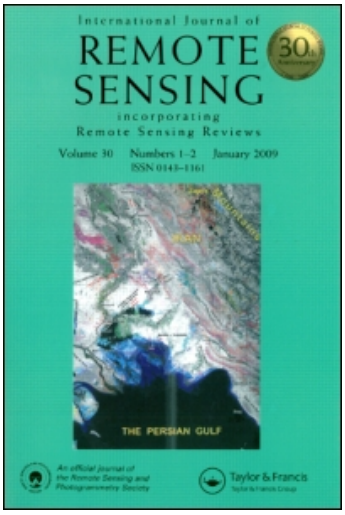

International Journal of Remote Sensing
Publication details, including instructions for authors and subscription information:
http://www.informaworld.com/smpp/title~content=t713722504

Water balance of the Arctic drainage system using GRACE gravimetry products

Frederic Frappart[a]; Guillaume Ramillien **[b]; James S. Famiglietti[a]
[a] Department of Earth System Science, University of California, Irvine, Croul Hall Irvine, CA, USA [b] Dynamique Terrestre et Planétaire (DTP), Observation Midi-Pyrénées, Toulouse, France

Online publication date: 06 February 2011

To cite this Article Frappart, Frederic , Ramillien **, Guillaume and Famiglietti, James S.(2011) 'Water balance of the Arctic drainage system using GRACE gravimetry products', International Journal of Remote Sensing, 32: 2, 431 — 453
To link to this Article: DOI: 10.1080/01431160903474954
URL: http://dx.doi.org/10.1080/01431160903474954

International Journal of Remote Sensing
Vol. 32, No. 2, 20 January 2011, 431–453

Taylor & Francis
Taylor & Francis Group

Water balance of the Arctic drainage system using GRACE gravimetry products

FREDERIC FRAPPART*†, GUILLAUME RAMILLIEN**‡ and JAMES S. FAMIGLIETTI†

†Department of Earth System Science, University of California, Irvine, Croul Hall Irvine, CA 92697-3100, USA

‡Dynamique Terrestre et Planétaire (DTP), Observation Midi-Pyrénées, UMR 5562, CNES/CNRS/IRD/UPS, 14 Av. Edouard Belin, 31400 Toulouse, France

(*Received 23 March 2009; in final form 6 November 2009*)

Land water and snow mass anomalies versus time were computed from the inversion of 50 Gravity Recovery and Climate Experiment (GRACE) geoids (August 2002 to February 2007) from the RL04 GeoForschungZentrum (GFZ) release and used to characterize the hydrology of the Arctic drainage system. GRACE-based time series have been compared to snow water equivalent and snow depth climatologies, and snowfall for validation purpose. Time series of regional averages of water volume were estimated for the 11 largest Peri-Arctic basins. Strong correlations were found between the snow estimates and river discharges in the Arctic basins (0.49–0.8). Then changes in land water storage were compared to precipitation minus evapotranspiration fluxes to determine which flux of the hydrological budget controls the Arctic hydrology. Results are very contrasted according to the basin. Trends of snow and land water masses were also computed over the 2003–2006 period. Eurasian basins lose snow mass whereas North American basins are gaining mass.

1. Introduction

The Arctic region is a major component of the global climate system and is expected to be significantly affected by global warming (Peterson *et al.* 2002). Although the Arctic Ocean holds only 1% of the global volume of seawater, it receives 11% of the world's freshwater input (Lammers *et al.* 2001). Arctic river discharges contribute 50% to the net flux of freshwater into the Arctic Ocean (Barry and Serreze 2000). Arctic hydrological systems exhibit large temporal variability caused by large-scale changes in atmospheric circulation (Proshutinsky *et al.* 1999). Discharge observations indicate a significant increase in Arctic discharge since the mid-1930s, with an acceleration in recent decades (Peterson *et al.* 2002, Serreze *et al.* 2003, McClelland *et al.* 2004, Stocker and Raible 2005). Timing and magnitude of northern river streamflow

*Corresponding author, at: Université de Toulouse, CNRS/IRD/OMP/LMTG, 14 Av. Edouard Belin, 31400 Toulouse, France, Email: frederic.frappart@lmtg.obs-mip.fr
**Now at Université de Toulouse, CNES/IRD/OMP/LMTG, 14 Av. Edouard Belin, 31400 Toulouse, France

International Journal of Remote Sensing
ISSN 0143-1161 print/ISSN 1366-5901 online
http://www.tandf.co.uk/journals
DOI: 10.1080/01431160903474954

are mostly influenced by winter snow mass storage and its subsequent melt (Rango 1997, Cao *et al.* 2002, Yang *et al.* 2003, 2007, 2009, Déry *et al.* 2005, Dyer 2008). The snow melt and associated floods during the spring/summer period comprise the most important hydrologic event of the year in the northern river basins (Cao *et al.* 2002, Yang *et al.* 2003). Changes in pattern of snow cover at high latitudes, such as the earlier start of snowmelt associated with warming in winter and spring seasons (Lammers *et al.* 2001, Kitaev *et al.* 2005, Groisman *et al.* 2006, Bulygina *et al.* 2007), may accentuate the variability of hydrologic regime at high latitudes in the context of global warming (Barnett *et al.* 2005).

The launch of the Gravity Recovery and Climate Experiment (GRACE) space mission in March 2002 enables, for the first time, detection of tiny temporal variations in Earth's gravity field (Tapley *et al.* 2004a, b), which over land are mainly due to the vertically-integrated water mass changes inside aquifers, soil, surface reservoirs and the snow pack, if effects of noise and residual errors from correcting models for atmosphere and ocean masses are neglected (Wahr *et al.* 1998, Rodell and Famiglietti 1999, Swenson *et al.* 2003). Wahr *et al.* (2006) showed that GRACE data over the continents provide information on the total land water storage with an accuracy of 15–20 mm of water thickness, equivalent to a spatial Gaussian average with a radius of 400 km. Ramillien *et al.* (2005) used an iterative inverse approach to estimate variations in continental water storage (i.e. all of the groundwater, soil water, surface water, snow and ice) and separate land waters and snow components from the GRACE RL02 data. Comparisons with model outputs and microwave observations have already demonstrated the quality of RL03 and RL02 land water and snow solutions derived by inverse method (Ramillien *et al.* 2005, 2006, Frappart *et al.* 2006). In a recent study, Niu *et al.* (2007) showed that the spatial pattern of snow derived from GRACE has a better agreement with climatologies than passive microwave estimates.

Our goal is to study the consistency of the snow mass variations derived from GRACE in terms of spatial and temporal patterns. In this study, we will be able, for the first time, to compare direct measurements of total land water and snow storages with river discharges in the Arctic drainage system. Previously, Syed *et al.* (2007) estimated river discharge from several Arctic basins, and compared GRACE-derived land water storage (but not separated snow storage) to observed and estimated discharge. In the present work, we more directly characterize the relationship between total land water, snow storage and river discharge. We use the RL04 GRACE land water and snow solutions computed using the method developed by Ramillien *et al.* (2005, 2006) to estimate time series of basin-scale land water and snow volume anomalies. We present estimates of snow water equivalent (SWE) and terrestrial water storage (TWS) anomalies from August 2002 to February 2007 for the 11 largest Arctic drainage basins, that is, Yukon, Mackenzie, Nelson, Severnyy Dvina, Pechora, Ob, Yenisey, Kotya, Lena, Indigirka and Kolyma (figure 1). We validated the GRACE-derived snow solutions by comparing them with pan-Arctic snow depth climatologies from USAF/ETAC (United States Air Force/Environmental Technical Applications Center) and the Arctic Climatology Project, a SWE climatology over North America and snowfall. While previous work has focused on the relationship between snow extent or depth and river run-off (Yang *et al.* 2003, Déry *et al.* 2005, Grippa *et al.* 2005), we compare continental water storage and snow volume variations derived from the inversion of GRACE geoids to *in situ* discharge for the largest Arctic river basins.

Figure 1. Location of the main Arctic drainage basins and their annual discharge ($km^3\ yr^{-1}$). Source: CAFF (2001), *Arctic Flora and Fauna: Status and Conservation. Conservation of Arctic Flora and Fauna* (Helsinki: Edita). Available at: http://maps.grida.no/go/graphic/major_river_systems_in_the_arctic.

2. Datasets

2.1 *GRACE-derived land water and snow mass solutions*

We use the monthly land water and snow solutions derived from the inversion of 50 GRACE geoids from the fourth data release by GeoForschungZentrum (GFZ-RL04), as presented in Ramillien *et al.* (2005, 2006). These solutions range from August 2002 to February 2007, with a few missing months (September and December 2002, January, June and July 2003, January 2004). They represent anomaly of mass expressed in terms of equivalent water thickness.

The GRACE-based land water and snow solutions separately computed in Ramillien *et al.* (2005) are spherical harmonics of a surface density function $F(\theta, \lambda, k)$ that represents the global map of either land waters or snow mass

$$F(\theta,\lambda,k)=\sum_{n=1}^{N}\sum_{m=0}^{n}\left[C_{nm}^{F}(k)\cos(m\lambda)+S_{nm}^{F}(k)\sin(m\lambda)\right]\widetilde{P}_{nm}(\cos\theta), \quad (1)$$

where θ and λ are co-latitude and longitude, k is the number of a given monthly solution, n and m are degree and order, $\widetilde{P}_{nm}$ is the associated Legendre function and $C_{nm}^{F}(t)$ and $S_{nm}^{F}(t)$ are the normalized water (or snow) mass coefficients (units: mm of equivalent water height) which were estimated by inversion (Ramillien *et al.* 2005). In practice, the spherical harmonic development cut-off N used for the land water solutions is limited to degree $N = 50$. This corresponds to a spatial resolution of ~400 km at the surface of the Earth. The GRACE-based land water and snow maps were interpolated on $1^\circ \times 1^\circ$ regular grids.

2.2 *Snow depth climatologies*

2.2.1 Global snow depth multi-year average. USAF/ETAC climatology is a $1^\circ \times 1^\circ$ monthly gridded dataset composed of snow depths averaged over an approximately 30-year window ending in the 1980s. The data come from various sources with varying degrees of accuracy, and were manually edited and interpolated using relatively simple methods (Foster and Davy 1988).

2.2.2 US–Russian snow depth climatology. The Environmental Working Group (EWG) Climatology Project compiled data on Arctic regions to expand scientific understanding of the Arctic and edited a set of complementary atlases for Arctic oceanography, sea-ice and meteorology, under the framework of the US–Russian Joint Commission on Economics and Technological Cooperation (Fetterer and Radionov 2000). The snow climatology is a gridded dataset in American Standard Code for Information Interchange Equal-Area Scalable Earth (ASCII EASE) grid format with a cell size of 250 km of monthly mean snow depth fields over the period 1966–1982.

2.2.3 Gridded monthly SWE climatology over North America. The Canadian Meteorological Service developed an operational snow depth analysis scheme which uses extensive daily snow depth observations from Canada and the USA to generate grids of snow depths and SWE at a resolution of 0.25° (Brassnet 1999). The monthly climatology grids were derived from daily snow depth and SWE grids covering the hydrological years 1979/80 to 1996/97. The gridded output is dominated by observations south of about 55° N. North of 55° N, the output is dominated by the snow model. SWE was estimated using the density values simulated by the snow model (Brown *et al.* 2003).

2.3 *Snowfall derived from GPCP rainfall*

The Global Precipitation Climatology Project (GPCP), established in 1986 by the World Climate Research Program, provides data that quantify the distribution of precipitation over the whole globe (Adler *et al.* 2003). We use here the Satellite-Gauge Combined Precipitation Data product of GPCP Version 2 data for evaluating our estimates of monthly SWE variations in the pan-Arctic region. The GPCP products we are using are monthly means with a spatial resolution of 1° of latitude and longitude and are available from January 1979 to present. Over land surfaces, the uncertainty in the rate estimates from GPCP is generally lower than over the oceans due to the *in situ* gauge input (in addition to satellite) from the GPCC (Global Precipitation

Climatology Center). Over land, validation experiments have been conducted in a variety of locations worldwide and suggest that while there are known problems in regions of persistent convective precipitation, non-precipitating cirrus or regions of complex terrain, the estimated uncertainties range between 10% and 30% (Adler *et al.* 2003).

Monthly snowfall is estimated from GPCP rainfall using the National Centers for Environmental Prediction (NCEP) air temperature topographically adjusted (available from the Arctic Rims website: http://rims.unh.edu/) according to the following equation:

$$\underline{P}_{snow} = \underline{P}_{tot}\underline{\theta}(\underline{T}_0 - \underline{T}) with\ \underline{\theta} = \begin{cases} 0\ if\ \underline{T} > \underline{T}_0 = 2^\circ C \\ \frac{\underline{T}_0 - \underline{T}}{2}\ if\ 0 < \underline{T} < \underline{T}_0 \\ 1\ if\ \underline{T} > 0 \end{cases}, \quad (2)$$

where P_{snow} is the estimated snowfall, P_{tot} is the GPCP rainfall, θ is a threshold function of air temperature, T the air temperature and T_0 the threshold air temperature (0°C).

2.4 *Snow outputs from WGHM model*

The WaterGAP Global Hydrology Model (WGHM) computes 0.5° × 0.5° gridded time series of monthly run-off and river discharge and is tuned against time series of annual river discharges measured at 724 globally distributed stations (Döll *et al.* 2003). It also provides monthly grids of snow and soil water. The effect of snow is simulated by a simple degree-day algorithm. Below 0°C precipitation falls as snow and is added to snow storage. Above 0°C, snow melts with a rate of 2 mm day^{-1} per degree in forests and 4 mm day^{-1} in case of other land cover types. These monthly gridded data are available from January 2002 to June 2006.

2.5 *River discharge measurements*

The monthly river discharge measurements at the closest station to the mouth of each basin were obtained at the Arctic RIMS (Rapid Integrated Monitoring System) website (ArcticRIMS 2003) for the 11 largest peri-Arctic drainage basins. This system has developed a near-real time monitoring of pan-Arctic water budgets and river discharge to the Arctic Ocean. The availability of the data for each basin is reported in table 1.

2.6 *Precipitation minus evapotranspiration dataset*

This dataset provides estimates of a monthly precipitation minus evapotranspiration (P-E) parameter using wind and humidity data from the NCEP/National Center for Atmospheric Research (NCAR) reanalysis with the 'aerological method' developed by Kalnay *et al.* (1996). The P-E parameter is equivalent to the vertically-integrated vapour flux convergence adjusted by the time change in precipitable water. On monthly timescales, P-E is dominated by the flux convergence term. NCEP/NCAR archives of vertical integrals of the monthly mean zonal and meridional fluxes and precipitable water (based on 6-hourly values at sigma levels), are used to compute the flux differences. The P-E fields are interpolated to the 25 km EASE grid. Details of the P-E calculations and some climate applications are provided by Cullather *et al.* (2000) and Serreze *et al.* (2003).

Table 1. Surface of the largest Arctic drainage basins (ArcticRIMS 2003), mean annual discharges (CAFF 2001) and availability of the discharges data at the closest station to the mouth.

Basin	Surface (km^2)	Mean annual discharge ($km^3\ yr^{-1}$)	Availability of river discharges at the closest station to the mouth
Yukon	833232	210	Not available
Mackenzie	1783972	340	2002–2005
Nelson	1106578	75	Not available
Severnyy Dvina	448664	110	1881–2009
Pechora	321731	140	1916–1998
Ob	2994238	530	1936–2009
Yenisey	2537404	603	1936–2009
Kotya (Kathanga)	372001	105	Not available
Lena	2460742	525	2000–2009
Indigirka	324244	57	1936–1998
Kolyma	651631	132	1978–2009

2.7 *Post-glacial rebound model*

Post-glacial rebound (PGR) designates the rise of land masses that were depressed by the huge weight of ice sheets during the last glacial period that ended between 10 000 and 15 000 years ago. It corresponds to a vertical elevation of the crust which happens especially in Scandinavia, the Hudson Bay in Canada (and maybe Antarctica) and affects the long wavelength components of the gravity field.

The PGR model used in this study is made available by the GRACE Tellus website (http://grace.jpl.nasa.gov). This model is based on the study by Paulson *et al.* (2007) and uses the global ICE-5G deglaciation model of Peltier (2004). It assumes an incompressible, self-gravitating Earth. The mantle is a Maxwell solid, and overlies an inviscid core. More details on ICE-5G can be found in Peltier (2004). Effects of a dynamic ocean response through the sea level equation were included using the formulation of polar wander described by Mitrovica *et al.* (2005). The uncertainty of its estimates is supposed to be around 20% (Paulson *et al.* 2007).

The GRACE Tellus website provides estimates of the rate of change of surface mass, expressed in mm yr^{-1} of equivalent water thickness. Degree-one terms were omitted when computing the mass because they are not included in the GRACE solutions. The results were smoothed using a Gaussian averaging function of 500 km radius. The mass estimates are provided on a $1^\circ \times 1^\circ$ grid, spaced 0.5° apart.

3. Validation of the GRACE-based snow water equivalent

3.1 *Annual cycle of GRACE-based SWE and comparisons with climatologies and GPCP-derived snowfall*

From the series of SWE anomaly grids derived from GRACE (using equation (1)), the temporal trend, seasonal and semi-annual amplitudes were simultaneously fitted by least-square adjustment at each grid point. We assumed that, at first order, the changes of SWE $\delta q(t)$ at each grid point are the sum of: a linear trend; an annual sinusoid, the pulsation of which is

$$\omega_{\text{ann}} = \frac{2\pi}{T_{\text{ann}}}, \tag{3}$$

where T_{ann} is ~1 year; a semi-annual sinusoid, the pulsation of which is:

$$\omega_{\text{semi-ann}} = \frac{2\pi}{T_{\text{semi-ann}}}, \tag{4}$$

where $T_{\text{semi-ann}}$ is ~6 months; and water mass residuals $\delta q^{\text{RES}}(t)$. This produces

$$\delta q(t) = At + B + C\cos(\omega_{\text{ann}} t + \varphi_{\text{ann}}) + D\cos(\omega_{\text{semi-ann}} t + \varphi_{\text{semi-ann}}) + \delta q^{\text{RES}}. \tag{5}$$

The parameters which we adjusted for each grid point (θ, λ) are the linear trend (i.e. slope A and y-intercept B), the annual cycle (i.e. amplitude C and phase φ_{ann}) and the semi-annual cycle (i.e. amplitude D and phase $\varphi_{\text{semi-ann}}$). For this purpose, we used a least-square fitting to solve the system

$$\boldsymbol{\delta Q} = \boldsymbol{\Phi}.X, \tag{6}$$

where the vector $\boldsymbol{\delta Q}$ is the list of the SWE values, $\boldsymbol{\Phi}$ and $\boldsymbol{X}$ are the configuration matrix and the parameter vector, respectively. The latter two terms are

$$\{\boldsymbol{\Phi}_j\} = \left[\, t_j \quad 1 \quad \cos(\omega_{\text{ann}} t_j) \quad \sin(\omega_{\text{ann}} t_j) \quad \cos(\omega_{\text{semi-ann}} t_j) \quad \sin(\omega_{\text{semi-ann}} t_j) \,\right] \tag{7a}$$

$$\boldsymbol{X} = [\alpha\, \beta\, \xi_{\text{ann}} \cos\varphi_{\text{ann}} - \xi_{\text{ann}} \sin\varphi_{\text{ann}}\ \xi_{\text{semi-ann}} \cos\varphi_{\text{semi-ann}} - \xi_{\text{semi-ann}} \sin\varphi_{\text{semi-ann}}] \tag{7b}$$

for adjusting the temporal trend and for fitting the annual and semi-annual amplitude and phase, where $\{\boldsymbol{\Phi}_j\}$ is the j^{th} line of the matrix $\boldsymbol{\Phi}$.

According to the least-square criteria, the solution vector of the system is

$$\boldsymbol{X}^{SOL} = (\boldsymbol{\Phi}^T \boldsymbol{\Phi})^{-1} \boldsymbol{\Phi}^T \boldsymbol{\delta Q}. \tag{8}$$

To locate the regions of snow accumulation, we focused on the annual cycle of SWE at high latitudes. Figure 2(*a*) presents the map of amplitude of annual cycle of SWE derived from the inversion of four years (2003–2006) of GRACE geoids. The two largest maxima of annual amplitude (~100 mm) are located over North America in the northern part of the Rocky Mountains and the western part of Canada. Over Eurasia, maximal amplitudes (70–90 mm) are observed in the eastern part of the Ob, Yenisey basins and the Kolyma basins. Secondary maxima, reaching 60 mm of SWE, are present in the western part of the Eurasian continent (Scandinavia, Severnyy Dvina, Pechora and the western part of the Ob basins).

Due to the coarse spatial and temporal resolutions (respectively 400 km and one month) of the GRACE-derived snow mass estimates, an indirect validation has been made using climatologies of snow depth from USAF/ETAC and EWG and snowfall-derived from GPCP rainfall products over North America and Eurasia, and a climatology of SWE over North America.

Figure 2 also presents the mean map of annual snow depth from USAF/ETAC (figure 2(*b*)) and EWG (figure 2(*c*)) climatologies, and the total annual snowfall derived from GPCP rainfall over the 2003–2006 period (figure 2(*d*)). The characteristics of these datasets are summarized in table 2. For comparison purpose, all the datasets have been resampled to a spatial resolution of 1°. The amplitude of annual cycles of GRACE-derived SWE, snow depth from both climatologies and snowfall derived from GPCP show similar patterns. The linear correlation coefficients between the GRACE

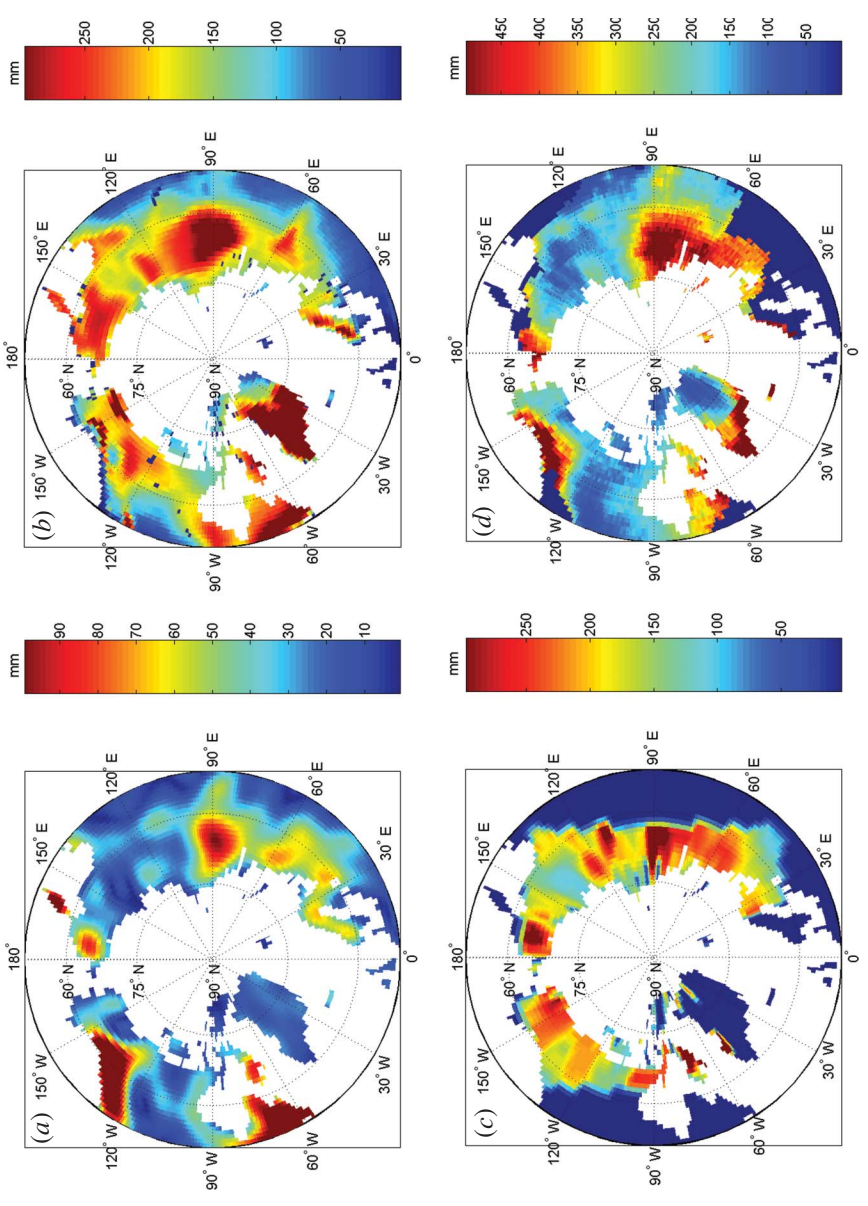

Figure 2. Maps of (*a*) SWE amplitude of annual cycle derived from GRACE over the 2003–2006 period; (*b*) mean annual snow depth from the ETAC monthly snow climatology; (*c*) mean annual snow depth from the EWG monthly snow climatology; and (*d*) total annual snowfall derived from GPCP rainfall over the 2003–2006 period.

Table 2. Spatial and temporal resolutions, and period acquisition of the GRACE-derived SWE and of the datasets used for comparisons.

Dataset	Spatial resolution	Temporal resolution	Acquisition period
GRACE-derived SWE	400 km	Monthly	2002–2007
USAF/ETAC snow depth climatology	1°	Monthly	1950s–1980s
EWG snow depth climatology	250 km	Monthly	1966–1982
CMS SWE climatology	0.25°	Monthly	1979–1997
GPCP-derived snowfall	1°	Monthly	2002–2007

amplitude of annual cycle, the mean annual snow depths from USAF/ETAC and EWG, and the total snowfall derived from GPCP, are respectively 0.53, 0.42 and 0.37. A strong signal can be observed on Eastern Canada (Newfoundland, Labrador and Baffin Island), Scandinavia, river basins in the European part of Russia (Severnyy Dvina and Pechora) and the Yenisey basin on all the datasets. Conversely, locations of snow accumulation are quite different between GRACE-derived SWE and snow depth climatologies in North-West Canada and East Siberia. Over North America, snow depth climatologies present a strong signal in Alaska and Yukon, Mackenzie and Nelson basins whereas GRACE-derived SWE has a strong maximum in the Rocky Mountains. Over Eurasia, USAF/ETAC snow climatology presents large snow depths in East Siberia (Kotia, Lena, Indigirka and Kolyma basins), EWG has the same pattern except for Indigirka basin, whereas GRACE-derived SWE presents lower snow accumulations over these regions. Two factors can explain these differences: the time periods considered (1950–1980 for USAF/ETAC climatology, 1966–1982 for EWG climatology, and 2003–2006 for both GRACE-derived SWE and GPCP-derived snowfall) in regions which have a strong response to climate variability; and the quantities compared related to snow density, which exhibits strong variability both in space and time.

Figure 3 displays the months with the maximum of the GRACE-derived SWE and snow depth from climatologies. Similar patterns can be observed on the three maps, especially a north–south gradient with maximum of snow occurring later in the north than in the south. The major difference lies in maxima occurring sooner in most of Siberia, Alaska and the North of the Rocky Mountains in the GRACE-derived SWE than in the snow depth climatologies. This is in accordance with the decrease of snow cover observed over Siberia between 1956 and 2004. This decrease was especially strong over central Siberia in late spring (April–May) for the period 1956–1991 (Groisman *et al.* 2006).

GRACE-derived SWE and the monthly mean climatology over North America were compared. Figure 4 shows the amplitude of the annual cycle of GRACE-derived SWE and the mean annual value of the SWE climatology. Both spatial pattern and intensity are very similar between the two products with a correlation coefficient of 0.58. The major difference is the strong signal over Alaska, which is present in the climatology and lacking in the GRACE products. This difference can be explained by the sparse coverage of stations in this region (Brown *et al.* 2003) and the time period considered as an increase of 0.4°C for the mean winter temperature has been observed between 1977 and 2004 (Molnia *et al.* 2007) which caused a decrease in the depth of the snow cover in Alaska (Osterkamp 2005).

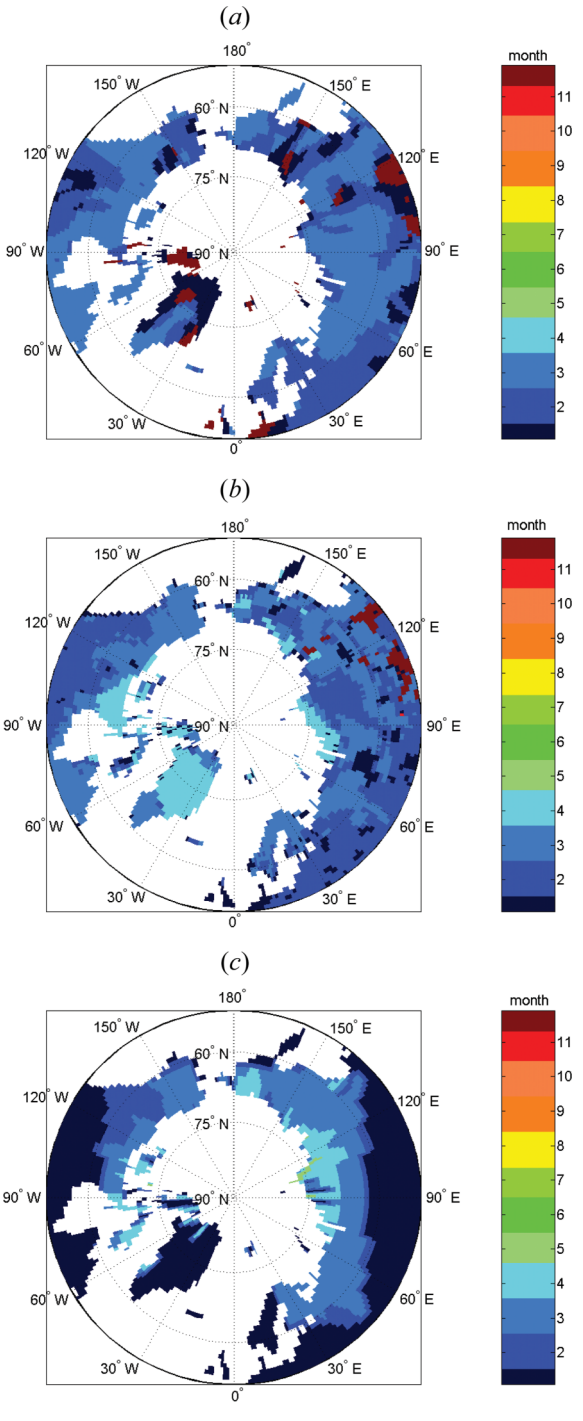

Figure 3. Months with (*a*) the maximum GRACE-derived SWE; (*b*) the snow depth from USAF/ETAC climatology; and (*c*) the snow depth from EWG climatology.

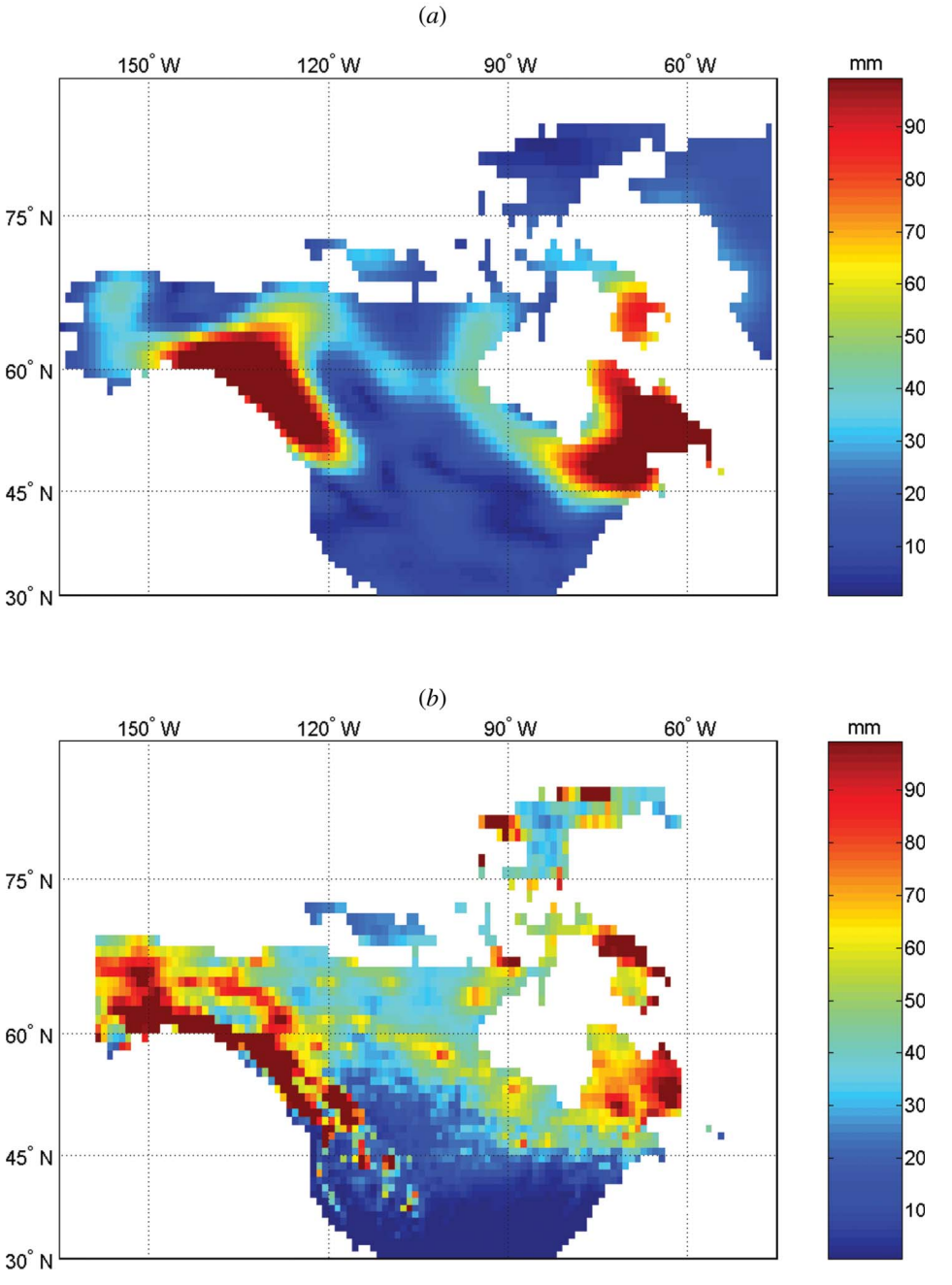

Figure 4. Maps of (*a*) SWE annual cycle derived from GRACE during the 2003–2006 period; and (*b*) mean annual SWE snow climatology over North America. Correlation = 0.58.

3.2 *Basin scale SWE time-series*

For a given month t, regional average of land water or snow volume (or height) $\delta V(t)$ ($\delta h(t)$ respectively) over a given river basin of area A is simply computed from the water height δh_j, with $j = 1, 2, \ldots$ (expressed in terms of mm of equivalent water height) inside A, and the elementary surface ${R_e}^2\ \delta\lambda\ \delta\theta\ \sin\theta_j$:

$$\delta V(t) = R_e^2 \sum_{j \in A} \delta h_j(\theta_j, \lambda_j, t) \sin\theta_j \delta\lambda\delta\theta \tag{9a}$$

$$\delta h(t) = \frac{R_e^2}{A} \sum_{j \in A} \delta h_j(\theta_j, \lambda_j, t) \sin\theta_j \delta\lambda\delta\theta, \tag{9b}$$

where θ_j and λ_j are co-latitude and longitude of the j^{th} element of surface, $\delta\lambda$ and $\delta\theta$ are the grid steps in longitude and latitude, respectively (generally $\delta\lambda = \delta\theta$). In practice, all points of A used in (equations (9a) and (9b)) are extracted for the 11 drainage basins masks at a 0.5° resolution provided by Oki and Sud (1998).

Figure 5 presents GRACE-based SWE time series for the four largest Arctic river basins (Ob, Yenisey, Lena and Mackenzie). In view of the short time span considered

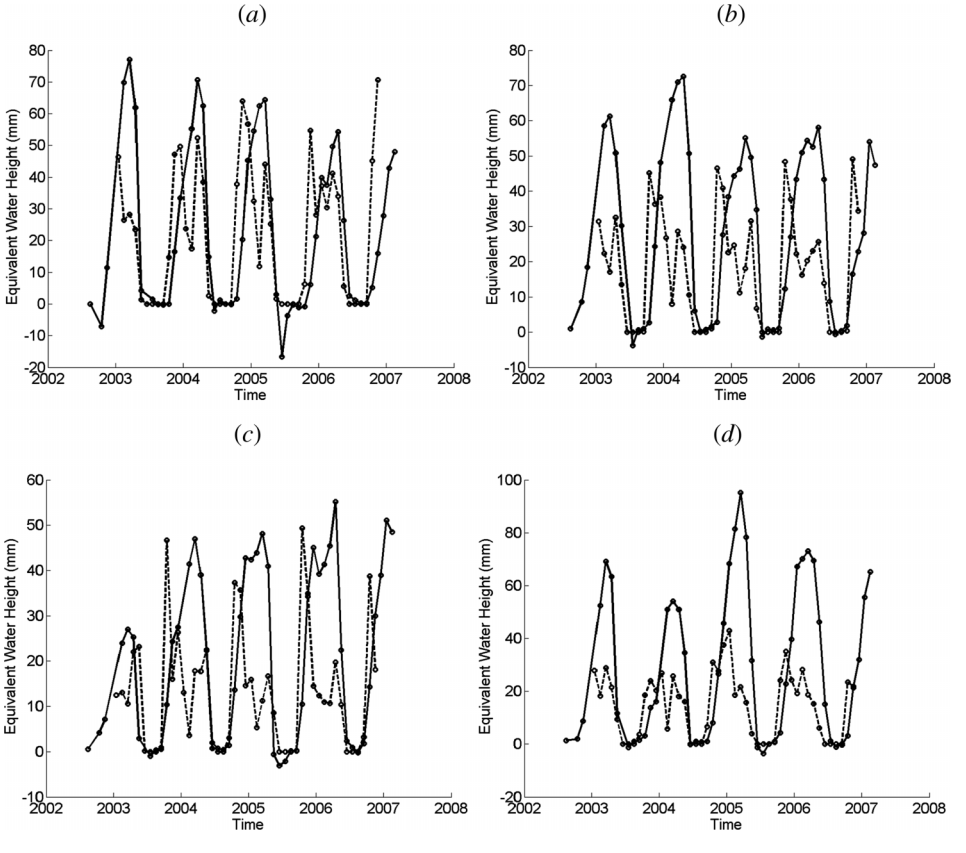

Figure 5. Time series of SWE derived from GRACE (continuous black) and snowfall derived from GPCP (dashed black) for the four largest Arctic drainage basins: (*a*) Ob, (*b*) Yenisey, (*c*) Lena, (*d*) Mackenzie.

here, the signal is dominated by the seasonal component with maxima of snow observed in February or March for all the basins. We estimated the correlation between the time series of GRACE-derived SWE and the time series of GPCP-derived snowfall for each basin, using the cross-correlation function:

$$\Gamma(t) = (S * D)(t) = \int_{\Delta t} S^*(\tau) D(\tau - t) \mathrm{d}\tau, \tag{10}$$

where Γ is the cross-correlation of the SWE S and the snowfall D at month t, τ is the time and Δt is the considered period of integration.

The time lag between snow and discharge peaks corresponds to the month t_0 that maximizes the cross-correlation function Γ:

$$\Gamma_{\max} = \Gamma(t_0) = \max_{t \in \Delta t}(\Gamma(t)), \tag{11}$$

where $\Gamma_{\max}$ is the maximum of Γ over the period Δt.

The results obtained are presented in table 3 for the maximum of correlation and the time lag between the peak of snowfall and the peak of SWE. For most of the basins, an agreement better than 40% is generally observed between snowfall and SWE (except for the Nelson basin). The time lags between snowfall and SWE never exceed two months. Due to the spatial resolution of GRACE products, the bigger the basin, the higher is the correlation (greater than 0.6, except for Lena). The exceptions are the Nelson and Indigirka basins where little or no SWE winter peak is observed in the GRACE-derived product. We compared the SWE derived from GRACE measurements with the SWE estimated by the WGHM model used as initial guess in the inverse method to extract the different hydrological components from GRACE data. For the Nelson and Indigirka basins, the amplitude of the snow signal from WGHM is also low (figure 6). Wahr *et al.* (2006) estimated that the accuracy of GRACE geoids is 15–20 mm water equivalent height for a spatial Gaussian average with a radius of 400 km. In these two cases, the monthly amplitude of the SWE signal is most of the time lower than 20 mm which represents the limit of detectability of a hydrological signal in the GRACE products.

Table 3. Correlation and time lag between GRACE-derived SWE and snowfall derived from GPCP by river basin.

GRACE/GPCP	Correlation	Time lag (months)
Yukon	0.75	2
Mackenzie	0.76	2
Nelson	0.11	0
Severnyy Dvina	0.57	1
Pechora	0.7	2
Ob	0.68	1
Yenisey	0.6	1
Kotya (Kathanga)	0.39	2
Lena	0.45	1
Indigirka	0.38	1
Kolyma	0.44	1

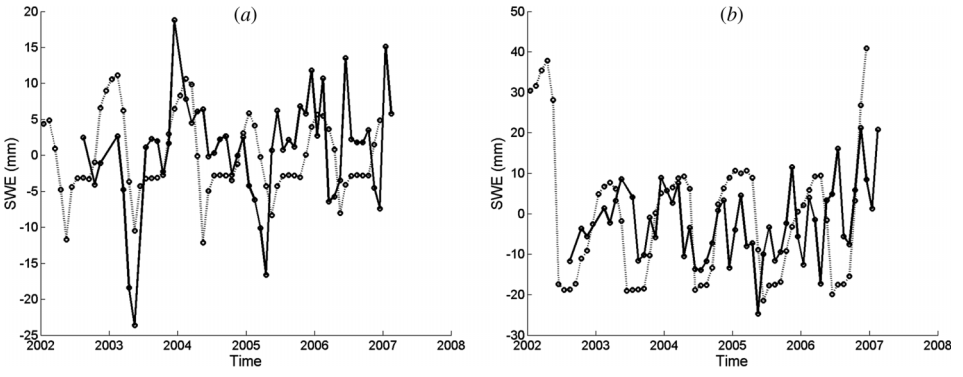

Figure 6. Time series of SWE derived from GRACE (black) and WGHM (dotted black) for the (*a*) Nelson and (*b*) Indigirka basins.

4. Analysis of water storage changes in the Arctic drainage system

4.1 *Basin scale TWS, snow and river discharge time series*

Figure 7 compares the monthly time series of SWE anomalies and TWS anomalies derived from GRACE measurements with the total water volume transferred to the Arctic Ocean for six Arctic drainage basins where river discharges measurements are available, that is Ob, Yenisey, Lena, Mackenzie, Severnaia Dvina and Kolyma. The total volume of water that flows from a basin to the Arctic Ocean each month is simply computed as the time integrated river discharge during the month.

Maxima of snow are observed in February or March for all the basins whereas maxima of land waters occurred generally one month later. These results tallied with those obtained by Dyer (2008) over the Yukon and Mackenzie basin with maximum of snow depth respectively occurring around day (55 ± 25) and (65 ± 15) over the periods 1975–2000 and 1972–2000. They are also in accordance with peak of SWE estimated using passive microwave observations for the Yukon (weeks 8–12), Ob (week 8), Lena and Yenisey (week 7) basins between 1988 and 2000 (Yang *et al.* 2007, 2009). We observe that snow mass represents the major part of the TWS. The discharge peak is observed in June except for the Severnaya Dvina basin where the discharge is maximum in May.

4.2 *Estimation of the correlation and time lag between SWE, TWS and river discharge*

To determine which reservoir, snow or total water, has the most significant effect on river discharge, we computed the cross-correlation function between the time series of TWS and snow component and the time series of integrated discharge for each drainage basin when river discharges are available. We estimated correlation between the time series of snow volume and the time series of integrated discharge for each basin, using the cross-correlation function (equation (10)) and the time lag between snow and discharge peaks corresponds to the month t_0 that maximizes the cross-correlation function (equation (11)).

The results obtained are presented in table 4 for the maximum of correlation and the time lag between the peak of land waters or snow and the peak of discharge. A good agreement between snow storage derived from GRACE and discharge is

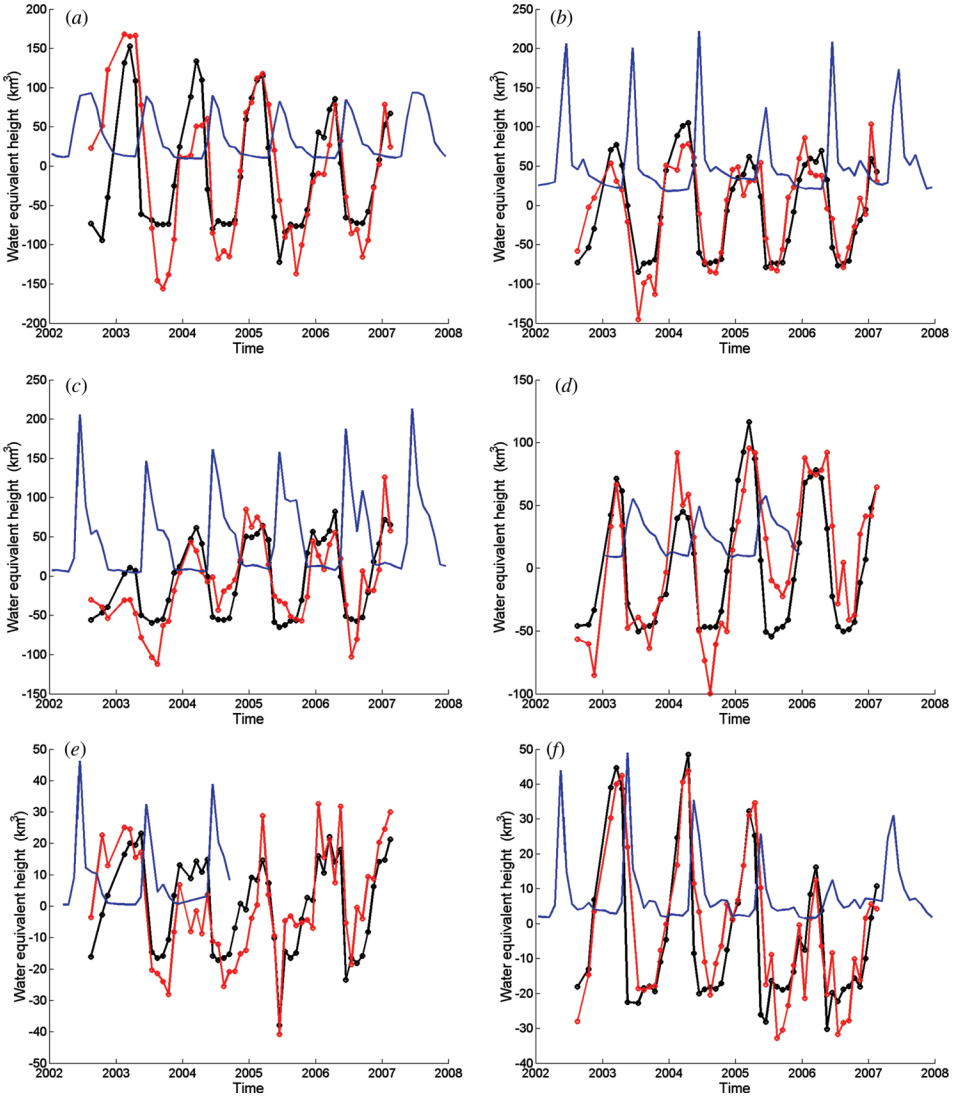

Figure 7. Time series of SWE (km^3) derived from GRACE (red), of TWS derived from GRACE (black) and of river discharges (blue) for the six Arctic drainage basins: (*a*) Ob, (*b*) Yenisey, (*c*) Lena, (*d*) Mackenzie, (*e*) Kolyma and (*f*) Severnaya Dvina.

observed for all the basins with correlation coefficients generally greater than 0.5 (table 4). For some basins, such as Lena, Mackenzie and Ob, the correlation is greater than 0.7. The correlation between TWS based on GRACE observations and discharge is lower whatever the basin you consider. For all the basins except Lena, correlations between snow mass and discharges and TWS and discharges are very close (the ratio between the correlation coefficients is greater than 0.75). In the case of the Lena basin, the correlation between snow storage from GRACE and river discharge is almost twice greater than the correlation between land water storage from GRACE and river discharge. These results are in accordance with the strong correlation observed

Table 4. Correlation and time lag between fresh water volume and snow stored for the different remote sensing datasets by river basin.

	GRACE (Land)/Discharge		GRACE (Snow)/Discharge	
	Correlation	Time lag (months)	Correlation	Time lag (months)
Kolyma	0.39	2	0.49	3
Lena	0.38	3	0.73	4
Mackenzie	0.66	3	0.77	4
Ob	0.65	3	0.8	4
Pechora	0.43	2	0.51	3
Svernaya Dvina	0.60	2	0.62	2
Yenisey	0.39	3	0.52	4

between runoff and P-E in the Lena watershed and the low correlation in the Mackenzie, Ob and Yenisey basins (Serreze *et al.* 2003).

The time lag between snow mass, TWS and river discharge is an important variable for describing the snow–run-off relationship as the snow stored during winter is not a direct indicator of the river flow during summer. Different hydrological factors can affect snow: after melting, the snow can evaporate, release as discharge, and be integrated to the interannual storage in ponds and wetlands (Bowling *et al.* 2003).

The results obtained seem to be consistent with river morphology: long time lags (greater than three months) are obtained for large drainage basins such as Lena, Mackenzie, Ob and Yenisey, and shorter time lags for smaller basins as Kolyma, Pechora and Severnaia Dvina. Some differences on the estimated time lags can be seen amongst the different datasets. They never exceed one month and can be caused by the monthly time sampling of the datasets. The results are in accordance with those obtained using Special Sensor Microwave Imager (SSM/I) by Grippa *et al.* (2005) over the 1989–2001 period which found a strong correlation between snow depth in February and run-off in June, for the Ob basin, consistent with the time lag of (19 ± 7) pentads between peak of snow volume and maximum discharge for the Mackenzie basin over 1972–2000 (Dyer 2008), of 15 or 16 weeks for the Ob basin and of 16 to 17 weeks for the Yenisey and Lena basins, between peaks of SWE derived from passive microwave observations and discharges over 1988–2000 (Yang *et al.* 2007).

4.3 *Interannual variability of GRACE-derived SWE*

The GRACE-derived SWE interannual variability has been analysed at basin scale. Maximum SWE has been estimated and compared to total annual discharge when the data are available. The results are presented in figure 8 for the Ob, Yenisey, Lena and Severnyy Dvina basins where data are available between 2003 and 2006. On the western part of the Eurasian continent, i.e. Severnyy Dvina, Pechora and Ob basins, there was a decline of both maximum SWE and total annual discharge. On the eastern part of Eurasia, the increase of SWE during winter 2004 is followed by a decrease in 2005. If a good agreement with river discharge is observed for the Lena basin, the increase of the total discharge increases one year before the increase of SWE in the Yenisey basin. This difference of behaviour is probably caused by the effect of melt of permafrost (which covers 90% of the surface of the Yenisey basin) and the influence of the dams on the seasonality of the discharge is strongest in this basin than in other

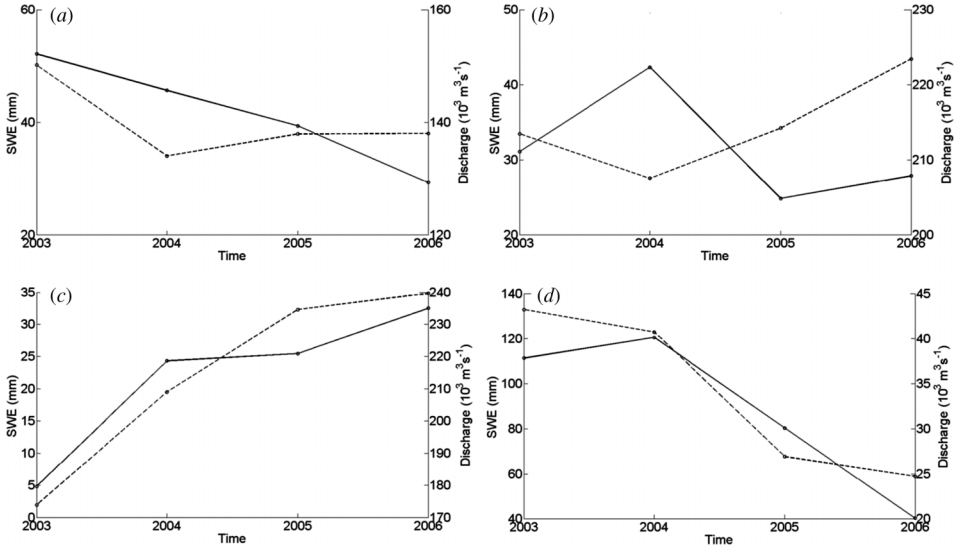

Figure 8. Time series of annual maximum of SWE derived from GRACE (black) and total annual discharge (dotted black) for (*a*) Ob, (*b*) Yenisey, (*c*) Lena and (*d*) Severnaia Dvina basins.

Eurasian basins (McClelland *et al*. 2004). In the Mackenzie basin (not shown), the mean winter SWE and annual river discharge present a similar time evolution: a decrease between 2003 and 2004 followed by an increase in 2005. The maximum SWE decreases between 2005 and 2006. In the Yukon basin (not shown), the maximum SWE remains constant between 2003 and 2004, before increasing in 2005 and decreasing in 2006.

4.4 *Basin-scale comparisons between GRACE-derived TWS and P-E*

The GRACE-derived TWS estimates can be compared to P-E through the instantaneous equation of the water mass balance applied to a watershed (see Hirschi *et al.* (2006), for instance):

$$\frac{\partial W}{\partial t} = P - E - R, \tag{12}$$

where $\frac{\partial W}{\partial t}$, P, E and R are water mass storage, precipitation rate, evapotranspiration rate and run-off, respectively. Time integration of equation (12) between times t_1 and t_2 (the starting and the ending dates of the considered period, with $\Delta t = t_2 - t_1$, assumed to be ~30 days, the average time span over which the GRACE geoids are provided) gives:

$$\Delta W = \Delta P - \Delta E - \Delta R, \tag{13}$$

where ΔW, ΔP, ΔE and ΔR are the monthly changes of the parameters of equation (12).

As no gridded run-off data were available for the Arctic region for the study period, we directly compare TWS changes with P-E for the 11 largest Arctic basins and cannot determine if the water budget is closed (i.e. equation (12) fully verified).

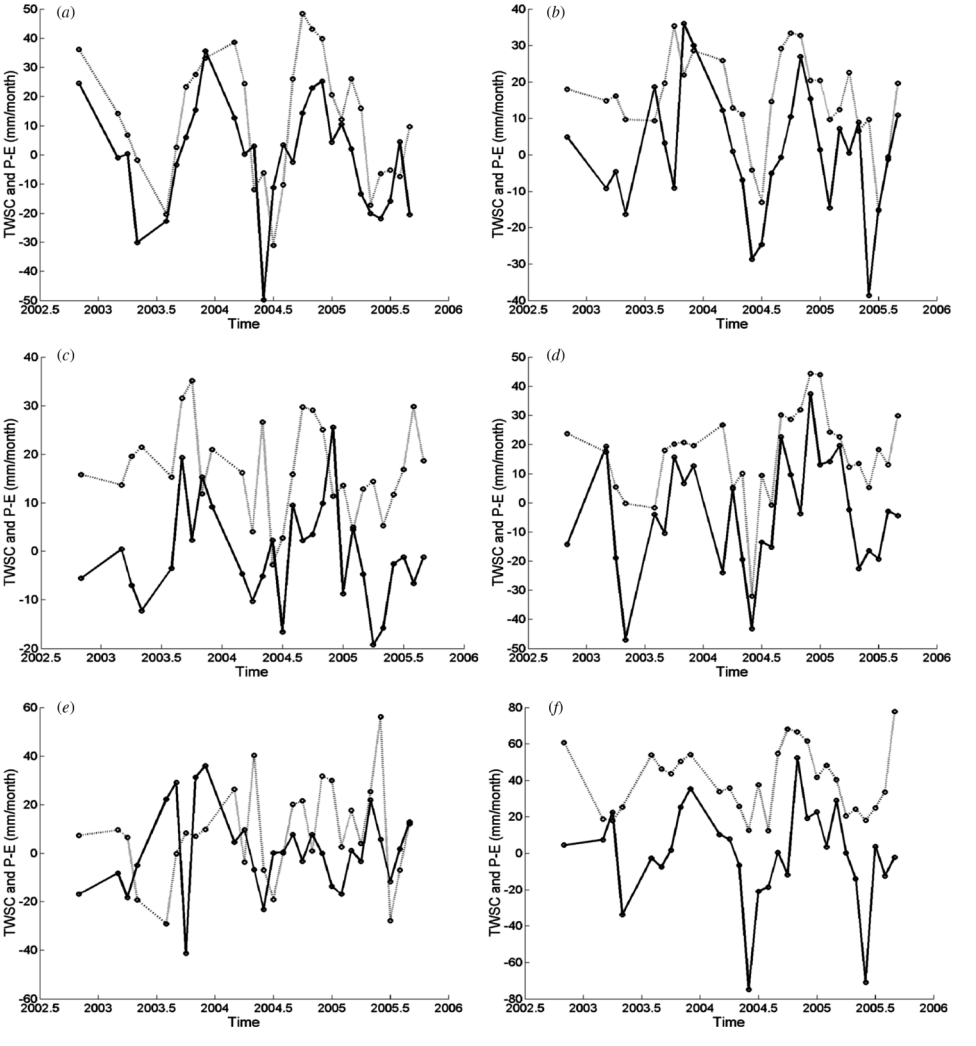

Figure 9. Time series of monthly TWS change derived from GRACE (black) and P-E (dotted black) for (*a*) Ob, (*b*) Yenisey, (*c*) Lena, (*d*) Mackenzie, (*e*) Nelson and (*f*) Yukon basins.

Time series of monthly changes of TWS and P-E are presented in figure 9. They generally present a similar evolution and range with respect to time, peaking during autumn in the northern hemisphere and reaching minima in May or June, in good accordance with climatologies (Serreze *et al.* 2003), except for Nelson where P-E is lower than the TWS change. The strong negative P-E anomaly of summer 2004, seen in most of the basins, is well observed in GRACE-derived TWS change.

Correlations between TWS change and P-E were computed and are reported in table 5. They allow us to determinate which fluxes most influence the TWS change. Three types of Arctic basins can be distinguished: (1) a strong influence of P-E on TWS change (i.e. correlation between TWS and P-E greater than 0.55) for the Ob, Yenisey and Mackenzie basins; (2) similar effect of P-E and run-off on TWS change (i.e. correlation between TWS and P-E greater than 0.5) for the Yukon, Severnaia

Table 5. Correlation between TWS and P-E by river basin.

Correlation	TWS/P-E
Yukon	0.48
Mackenzie	0.68
Nelson	0
Severnaia Dvina	0.51
Pechora	0.51
Ob	0.7
Yenisey	0.57
Kotya (Kathanga)	0.18
Lena	0.24
Indigirka	0.15
Kolyma	0.17

Dvina and Pechora basins and (3) run-off dominates TWS change (i.e. correlation between TWS and P-E lower than 0.3) for the Nelson, Kotya, Lena, Indigirka and Kolyma basins. Similar results were also found by Serreze *et al*. (2003) for the Ob, Yenisey, Lena and Mackenzie basins, comparing climatologies of P-E and run-off.

4.5 *Trends of SWE, TWS and river discharges*

Basin-scale trends of SWE, TWS, river discharges and PGR were estimated over 2003–2006 using equation 7(b). As the hydrological signals are not stationary, these trends are valid over the 2003–2006 period. The results are presented in table 6. PGR represents a possible source in our SWE and TWS trend estimates, as GRACE, which measures vertically integrated gravity, cannot distinguish between snow/water and other solid Earth signals. We used the global ICE-5G deglaciation model of Peltier (2004), modified by Paulson *et al.* (2007), to compute PGR trends in each watershed (cf. table 6). PGR has a very important effect over Canada (18.8 and 25.6 $km^3\ yr^{-1}$ for Nelson and Mackenzie basins, respectively) and also, but not as importantly and with the opposite sign, the large Siberian basins (–0.96, –0.77 and –0.59 $km^3\ yr^{-1}$ for Ob, Yenisey and Lena basins, respectively; for the other basins, the effect of PGR is lower

Table 6. Trends of snow volume, TWS volume and water volume to the Arctic Ocean (when data are available) estimated between 2003 and 2006 by river basin.

	Trend ($km^3\ yr^{-1}$)			
	SWE (GRACE)	TWS (GRACE)	Discharge	PGR
Yukon	1.8 ± 0.7	–7.3 ± 0.6	—	–0.01
Mackenzie	10.9 ± 1.0	18.5 ± 1.0	0.5 ± 0.5	25.60
Nelson	0.7 ± 0.2	4.5 ± 0.2	—	18.80
Severnaia Dvina	–4 ± 0.4	–6.4 ± 0.4	–1.6 ± 0.2	0.26
Pechora	–2 ± 0.3	–4.1 ± 0.3	—	–0.18
Ob	–5.7 ± 1.4	–10 ± 1.6	–0.8 ± 0.5	–0.96
Yenisey	–1.1 ± 1.4	7.9 ± 1.2	0.5 ± 1.5	–0.77
Kotya (Kathanga)	–2.1 ± 0.2	0.8 ± 0.2	—	–0.13
Lena	8.6 ± 0.9	13.6 ± 0.9	4.4 ± 0.9	–0.59
Indigirka	0.1 ± 0.1	1.1 ± 0.2	—	–0.17
Kolyma	–1.2 ± 0.3	3.4 ± 0.3	—	–0.31

than 0.3 $km^3\ yr^{-1}$ in absolute value). In case of error-free PGR modelling, the PGR effect should be subtracted from SWE and TWS trends. Unfortunately, PGR effects remain not so well modelled since there are still large uncertainties about the Earth's interior (e.g. the constant of viscosity between upper and lower mantles). So, we decided to present the results without PGR correction, as this suffers from significant errors itself (table 6). We notice that all the large Eurasian basins (except Indigirka where the inverse method gives unreliable results) considered in this study are losing snow mass, even in large amounts, such as for Lena ($-8.6 \pm 0.9\ km^3\ yr^{-1}$), Ob ($-5.7 \pm 1.4\ km^3\ yr^{-1}$) and Severnaia Dvina ($-4 \pm 0.4\ km^3\ yr^{-1}$). Conversely, all the large North American basins are gaining snow mass (even Nelson where the inverse method gives unreliable results), except if we consider the effect of the PGR. Even if complex hydrological mechanisms occurred after the snow melt (Bowling *et al.* 2003), increase (decrease) in snow mass could be explained by a decrease (increase) of snow melt, and as a consequence by a decrease (increase) of river discharges in North America (Eurasia respectively). This is in accordance with the large increase of the Eurasian river discharges and the small decrease of the North American river discharges (McClelland *et al.* 2004). Nevertheless, comparisons with *in situ* discharges data do not validate this assumption, as Mackenzie discharge is increasing by $0.5 \pm 0.5\ km^3\ yr^{-1}$ and Ob and Severnaia Dvina discharges are respectively decreasing by 0.8 ± 0.5 and $1.6 \pm 0.2\ km^3\ yr^{-1}$ over the same period. For the Mackenzie basin, due to the effect of the PGR, the SWE trend should be negative, and so the assumption should be verified. Trends of river discharges appear to be more correlated to trends in TWS. Moreover, Eurasia can be divided in two parts: the western part with negative trends for SWE, TWS and river discharges, and the eastern part with negative trends for SWE but positive trends for TWS and river discharges. In the northern hemisphere, Siberia was one of the regions most affected by the recent warming (Jones and Moberg 2003, Groisman and Bartalev 2004, Groisman *et al.* 2006; also see http://www.ncdc.noaa.gov/gcag/gcag.html). This warming is responsible for both a melt of the snow and of the permafrost. In western Eurasia where the permafrost only represents a small area and is discontinuous, TWS is mainly affected by decrease of SWE. Conversely, in eastern Eurasia where the permafrost is important, TWS could be recharged by a melt of the permafrost and TWS can increase, whereas SWE decreases.

5. Conclusion

For the first time, GRACE-derived hydrological products are used to provide a description of several hydrological processes related to snow in the Arctic drainage system. Comparisons between GRACE-derived SWE, and snow depth and SWE climatologies, show a relatively good agreement between the different products. In addition, comparisons between GRACE-derived SWE product and snowfall derived from GPCP rainfall over the same time period exhibit very similar spatial patterns (correlations of 0.75 have been reached for Yukon and Mackenzie basins) and interannual variations have well-correlated time variations at basin scale. The direct comparison at basin scales between snow mass variations, land water variations and river discharge time evolution shows that the snow component has a more significant impact on river discharge at high latitudes than TWS, corroborating the results found earlier by Yang *et al.* (2003); this suggests a strong linkage between snow cover extent and streamflow. Time lags between snow mass maxima and discharge peaks, consistent with the size of drainage basins, were also estimated. Interannual variability of SWE derived from GRACE is accordance with interannual variability of river

discharges for most of the drainage basins. These results contribute to a better understanding of the relationship between snow and discharge and for hydrological models parameterization.

This study also provides a characterization of the respective influence of P-E and R on the TWS change at high latitudes. Time correlation between TWS and P-E allows us to distinguish the drainage basins where TWS is dominated by P-E, equally influenced by P-E and run-off and mostly influenced by run-off.

The estimates of SWE and TWS trends over the 2003–2006 period showed that all the Eurasian basins lose snow mass whereas North American basins are gaining mass. Nevertheless, if we consider the effect of PGR, Mackenzie and Nelson basins also lose snow mass. In addition, Eurasia can be divided into two parts: the western part where both SWE and TWS are decreasing and the eastern part where SWE is decreasing but TWS is increasing. This different behaviour could be related to melt of the permafrost mostly present in eastern Eurasia.

Acknowledgements

The first and third authors were supported by NASA GRACE Science Team grant NG04GE99G and NASA REASoN grant JPL 1259524.

References

Adler, R.F., Huffman, G.J., Chang, A., Ferraro, R., Xie, P., Janowiak, J., Rudolf, B., Schneider, U., Curtis, S., Bolvin, D., Gruber, A.J., Susskind, J. and Arkin, P., 2003, The Version 2 Global Precipitation Climatology Project (GPCP) monthly precipitation analysis (1979–present). *Journal of Hydrometeorology*, **4**, pp. 1147–1167.

Arctic RIMS, 2003, A regional, integrated hydrological monitoring, system for the pan-Arctic land mass. Available online at: http://www.watsys.sr.unh.edu/arctic/RIMS/ (accessed 20 March 2009).

Barnett, T.P., Adam, J.C. and Lettenmeier, D.P., 2005, Potential impacts of a warming climate on water availability in snow-dominated regions. *Nature*, **438**, pp. 303–309.

Barry, R.G. and Serreze, M.C., 2000, Atmospheric components of the Arctic Ocean freshwater balance and their interannual variability. In *The Freshwater Budget of the Arctic Ocean*, E.L. Lewis, E.P. Jones, P. Lemke, T.D. Prowse and P. Wadhams (Eds.), NATO Science Series 2, Environmental Security, pp. 45–56 (Dordrecht, The Netherlands: Kluwer Academic).

Bowling, L.C., Kane, D.L., Gieck, R.E., Hinzman, L.D. and Lettenmeier, D.P., 2003, The role of surface storage in a low-gradient Artic watershed. *Water Resources Research*, **39**, p. 1087.

Brasnett, B., 1999, A global analysis of snow depth for numerical weather prediction. *Journal of Applied Meteorology*, **38**, pp. 726–740.

Brown, R.D., Brasnett, B. and Robinson, D., 2003, Gridded North American daily snow depth and snow water equivalent for GCM evaluation. *Atmosphere-Ocean*, **41**, pp. 1–14.

Bulygina, O.N., Razuvaev, V.N., Korshunova, N.N. and Groisman, P.Ya., 2007, Climate variations and changes in extreme climate events in Russia. *Environmental Research Letters*, **2**, p. 045019, doi: 10.1088/1748-9326/2/4/045020.

CAFF (Conservation of Arctic Flora and Fauna), 2001, *Arctic Flora and Fauna: Status and Conservation. Conservation of Arctic Flora and Fauna* (Helsinki: Edita).

Cao, Z., Wang, M., Proctor, B., Strong G., Stewart R., Ritchie, H. and Burford, J.E., 2002, On the physical processes associated with the water budget and discharge over the Mackenzie basin during the 1994/95 water year. *Atmosphere-Ocean*, **40**, pp. 125–143.

Cullather, R.I., Bromwich, D.H. and Serreze, M.C., 2000, The atmospheric hydrologic cycle over the Arctic basin from reanalyses. Part I: comparison with observations and previous studies. *Journal of Climate*, **13**, pp. 923–937.

Dery, S.J., Sheffield, J. and Wood, E.F., 2005, Connectivity between Eurasian and Canadian snow water equivalent and river discharge. *Journal of Geophysical Research*, **110**, p. D23106, doi: 10.1029/2005JD006173.

Döll, P., Kaspar, F. and Lehner, B., 2003. A global hydrological model for deriving water availability indicators: model tuning and validation. *Journal of Hydrology*, **270**, pp. 105–134.

Dyer, J., 2008, Snow depth and streamflow relationships in large North American watersheds. *Journal of Geophysical Research*, **113**, p. D18113, doi:10.129/2008JD010031.

Fetterer, F. and Radionov, V. (Eds.), 2000, *Arctic Climatology Project Environmental Working Group Arctic Meteorology and Climate Atlas* (Boulder, CO: National Snow and Ice Data Center). CD-ROM.

Foster, D.J. and Davy, R.D., 1988. Global snow depth climatology. USAF ETAC/TN-88/006, Scott Air Force Base, Illinois, p. 48.

Frappart, F., Ramillien, G., Biancamaria, S., Mognard, N.M. and Cazenave, A., 2006, Evolution of high-latitude snow mass derived from the GRACE gravimetry mission (2002–2004). *Geophysical Research Letters*, **33**, p. L02501, doi:10.1029/2005GL024778.

Grippa, M., Mognard, N.M. and Le Toan, T., 2005, Comparison between the interannual variability of snow parameters derived from SSM/I and the Ob river discharge. *Remote Sensing of Environment*, **98**, pp. 35–44.

Groisman, P. Ya. and Bartalev, S.A. (Eds.), 2004, *Northern Eurasia Earth Science Partnership Initiative (NEESPI) Science Plan*, prepared by the NEESPI Science Plan Development Team. Available online at: http://neespi.org (accessed 1 April 2009).

Groisman, P. Ya., Knight, R.W., Razuraev, V.N., Bulygina, O.N. and Karl, T.R., 2006, State of the ground: climatology and changes during the past 69 years over northern Eurasia for a rarely used measure of snow cover and frozen land. *Journal of Climate*, **19**, pp. 4933–4955.

Hirschi, M., Seneviratne, S.I. and Schar, C., 2006, Seasonal variations in terrestrial water storage for major midlatitude river basins, *Journal of Meteorology*, **7**, pp. 39–60.

Jones, P.D. and Moberg, A., 2003, Hemispheric and large-scale surface air temperature variations: an extensive revision and an update to 2001. *Journal of Climate*, **16**, pp. 206–223.

Kalnay, E., Kanamitsu, M., Kistler, R., Collins, W., Deaven, D., Gandin, L., Iredell, M., Saha, S., White, G., Woolen, J., Zhu, Y., Chelliah, M., Ebisuzaki, W., Higgens, W., Janowiak, J., Mo, K.C., Ropelewski, C., Wang, J., Leetma, A., Reynolds, R., Jenne, R. and Joseph, D., 1996, The NCEP/NCAR 40-year reanalysis project. *Bulletin of the American Meteorological Society*, **77**, pp. 437–471.

Kitaev, L., Førland, E., Razuvaev, V., Tveito, O.E. and Krueger, O., 2005, Distribution of snow cover over Northern Eurasia. *Nordic Hydrology*, **36**, pp. 311–319.

Lammers, R.B., Shiklomanov, A.I., Vorosmarty, C.J., Fekete, B.M. and Peterson, B.J., 2001, Assessment of contemporary Arctic river runoff based on observational discharge records. *Journal of Geophysical Research*, **106**, pp. 3321–3334.

McClelland, J.W., Holmes, R.M., Peterson, B.J. and Stieglitz, M., 2004, Increasing river discharge in the Eurasian Arctic: Consideration of dams, permafrost thaw, and fires as potential agent of change. *Journal of Geophysical Research*, **109**, p. D18102, doi: 10.1029/2004JD005483.

Mitrovica, J.X., Wahr, J., Matsuyama, I. and Paulson, A., 2005, The rotational stability of an Ice Age Earth. *Geophysical Journal International*, **161**, pp. 491–506.

Molnia, B.F., 2007, Late nineteenth to early twenty-first century behavior of Alaskan glaciers as indicators of changing regional climate. *Global Planetary Change*, **56**, pp. 23–56.

Niu, G.-Y., Seo, K-W. Yang, Z.-L., Wilson, C., Su, H., Chen, J. and Rodell, M., 2007, Retrieving snow mass from GRACE terrestrial water storage change with a land surface model. *Geophysical Research Letters*, **34**, p. L15704, doi:10.1029/2007GL030413.

Oki, T. and Sud, Y.C., 1998. Design of Total Runoff Integrating Pathways (TRIP) – a global river channel network. *Earth Interactions*, **2**, pp. 1–37.

OSTERKAMP, T.E., 2005. The recent warming of permafrost in Alaska. *Global Planetary Change*, **49**, pp. 187–202.

PAULSON, A., ZHONG, S. and WAHR, J., 2007, Inference of mantle viscosity from GRACE and relative sea level data, *Geophysical Journal International*, **171**, pp. 497–508.

PELTIER, W.R., 2004, Global glacial isostasy and the surface of the ice-age Earth: the ICE-5G(VM2) model and GRACE. *Annual Review of Earth and Planetary Sciences*, **32**, pp. 111–149.

PETERSON, B.J., HOLMES, R.M., MC CLELLAND, J.W., VOROSMARTY, C.J., LAMMERS, R.B., SHIKLOMANOV, A.I., SHIKLOMANOV, I.A. and RAHMSTORF, S., 2002, Increasing river discharge to the Arctic Ocean. *Science*, **298**, pp. 2171–2173.

PROSHUTINSKY, A., POLYAKOV, I. and JOHNSON, M., 1999, Climate states and variability of Arctic ice and water dynamics during 1946–1997. *Polar Research*, **18**, pp. 135–142.

RAMILLIEN, G., FRAPPART, F., CAZENAVE, A. and GUENTNER, A., 2005, Time variations of the land water storage from an inversion of 2 years of GRACE geoids. *Earth Planetary Science Letters*, **235**, pp. 283–301.

RAMILLIEN, G., FRAPPART, F., CAZENAVE, A., GUENTNER, A. and LAVAL, K., 2006, Time variations of the regional evapotranspiration rate from Gravity Recovery and Climate Experiment (GRACE) satellite gravimetry. *Water Resources Research*, **42**, W10403, doi: 10.1029/2005WR004331.

RANGO, A., 1997, Response of areal snow cover to climate change in a snowmelt-runoff model. *Annals of Glaciology*, **25**, pp. 232–236.

RODELL, M. and FAMIGLIETTI, J.S., 1999, Detectability of variations in continental water storage from satellite observations of the time dependent gravity field. *Water Resources Research*, **35**, pp. 2705–2723.

SERREZE, M.C., BROMWITCH, D.H., CLARK, M.P., ETRINGER, A.J., ZHANG, T. and LAMMERS, R.B., 2003, Large-scale hydro-climatology of the terrestrial Arctic drainage system, *Journal of Geophysical Research*, **108**, p. 8160, doi: 10.1029/2001JD000919.

STOCKER, T.F., and RAIBLE, C.C., 2005, Water cycle shifts gear. *Nature*, **434**, pp. 830–833.

SWENSON, S., WAHR, J. and MILLY, P.C.D., 2003, Estimated accuracies of regional water storage variations inferred from the Gravity Recovery and Climate Experiment (GRACE). *Water Resources Research*, **39**, p. 1223, doi:10.1029/2002WR001808.

SYED, T.H., FAMIGLIETTI, J.S., ZLOTNICKI, V. and RODELL, M., 2007, Contemporary estimates of Pan-Arctic freshwater discharge from GRACE and reanalysis. *Geophysical Research Letters*, **34**, p. L19404, doi:10.1029/2007GL031254.

TAPLEY, B.D., BETTADPUR, S., RIES, J., THOMPSON, P.F. and WATKINS, M., 2004a, GRACE measurements of mass variability in the Earth system. *Science*, **305**, pp. 503–505.

TAPLEY, B.D., BETTADPUR, S., WATKINS, M. and REIGBER, C., 2004b, The gravity recovery and climate experiment: mission overview and early results. *Geophysical Research Letters*, **31**, p. L09607, doi:10.1029/2004GL019920.

WAHR, J., SWENSON, S. and VELICOGNA, I., 2006, The accuracy of GRACE mass estimates. *Geophysical Research Letters*, **33**, L06401, doi:10.1029/2005GL025305.

WAHR, J.M., HAN, D. and TRUPIN, A., 1998, Time-variability of the Earth's gravity field: Hydrological and oceanic effects and their possible detection using GRACE. *Journal of Geophysical Research,* **103**, pp. 30 203–30 230, doi: 10.1029/98JB02844.

YANG, D., ROBINSON, D., ZAO, Y., ESTILOW, T. and YE, B., 2003, Streamflow response to seasonal snow cover extent changes in large Siberian watersheds. *Journal of Geophysical Research*, **108**, p. 4578, doi: 10.1029/2002JD003419.

YANG, D., ZHAO, Y., ARMSTRONG, R. and ROBINSON, D., 2009, Yukon river streamflow response to seasonal snow cover changes. *Hydrological Processes*, **23**, pp. 109–121.

YANG, D., ZHAO, Y., ARMSTRONG, R., ROBINSON, D. and BRODZIK, M.J., 2007, Steamflow response to seasonal snow cover mass changes over large Siberian watersheds. *Journal of Geophysical Research*, **112**, p. F02S22, doi: 10.129/2006JF000518.